PHOTOCURRENT EFFECTS IN AN ELECTROABSORPTION MODULATOR INTEGRATED WITH SGDBR LASER

L.A. Johansson, Y.A. Akulova*, G.A. Fish* and L.A. Coldren
Department of Electrical and Computer Engineering
University of California, Santa Barbara, CA 93106
Tel: (805) 893-4543, Fax: (805) 893-7500, email: leif@ece.ucsb.edu
*Agility Communications, Inc., 600 Pine Ave, Santa Barbara, CA 93117

Abstract – High photocurrent effects in an electroabsorption modulator are explored using the high output power from an integrated SGDBR laser followed by semiconductor optical amplifier. It is shown how the equivalent EAM junction resistance is reduced with photocurrent to lower than 30Ω, how the modulation response is correspondingly affected and how the gain of electroabsorption-modulated analog links ultimately becomes limited by the absorbed photocurrent.

I. Introduction

Electroabsorption modulators (EAMs) are currently being investigated for use in low-loss analog optical links [1]. Due to the large optical power required in an externally modulated link to achieve high link gain, high optical power effects in EAMs need to be investigated. MQW EAMs are usually chosen for use in low loss analog links because of the smaller driving voltage. However, the relatively low saturation power of MQW modulators limits the amount of optical power that can be coupled into the modulator and past investigations into the effect absorbed photocurrent are correspondingly limited to relatively small absorbed photocurrent close to the saturation power limit of the modulators [2]. A further constraint is to limit the input optical power to waveguide devices, not to cause surface damage to the input facet of the device [3].

We have previously shown how a large amount of optical power can be coupled into a bulk waveguide Franz-Keldysh effect (FKE) modulator by integration to an SGDBR laser and a semiconductor optical amplifier (SOA) [4]. Because of the high saturation power of the FKE modulator, a linear photocurrent up to 70 mA was observed with little sign of saturation. In this paper, we take advantage of the large waveguide optical power to investigate some of the limits that applies to an analog optical link using an EAM.

II. Device

The device is illustrated in Fig. 1 and consists of a sampled-grating DBR laser, an SOA, and an electroabsorption modulator, all integrated on the same InP chip. More than 10mW output power, lower than 2MHz linewidth, and more than 40dB sidemode suppression ratio has been achieved over more than 40nm wavelength tuning range [5]. Typical operation conditions for 10 mW CW are I_{gain} = 150 mA, I_{FM} and I_{RM} below 27 and 43 mA, respectively, and I_{SOA} below 150 mA. The bulk FKE modulator design allows improved power handling of the device, avoiding carrier pileup problems, up to a 200mW *I-V* product, *I* being the EAM photocurrent. The efficient coupling between the source and the modulator waveguide structure makes it convenient to study high optical power effects in the EAM device.

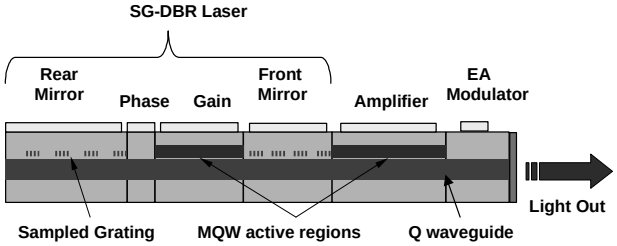

Fig 1. SGDBR-SOA-EAM Device Schematic

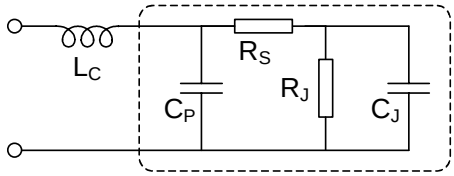

Fig. 2: EAM RF equivalent circuit model

The integrated electro-absorption modulator can be modeled using a simple equivalent circuit, shown in Fig. 3. R_J and C_J (0.5 pF) are the device junction capacitance and resistance, R_S (7Ω) is the device shunt resistance, L_C (0.8 nF) is the bondwire inductance and C_P (0.5 pF) is the bonding-pad capacitance. It has previously been demonstrated that the photocurrent can be modeled as an equivalent change in junction resistance [6].

III. Modulator performance

Figure 3 shows the complementary measurement of transmitted optical power and absorbed photocurrent in the modulator. The maximum slope of the photocurrent corresponds to an equivalent device impedance of 50Ω. The effect of the reduced impedance at higher optical power also affects the behavior of the modulator under modulation. Figure 4 shows S11 of the modulator at different optical power, taken at maximum slope efficiency. The input optical power into the modulator was regulated by changing the SOA bias current. It is seen that for 115 mA SOA bias current, an almost perfect 50Ω match is achieved. The dip in the S11 response above 10 GHz is caused by interaction between the bond-wire inductance and the capacitance at the AlN-substrate the device is mounted on. Fig. 5 shows the equivalent device conductance as a function of transmitted optical power, derived from the S11 data at low frequencies. It is seen that the conductance varies linearly with the optical power and can be as high as 0.029S, corresponding to the 7Ω shunt resistance in series with a junction resistance of only 27Ω. For electroabsorption modulators with higher available slope efficiency, such as offered by quantum-well modulators, the junction resistance would become even lower at a similar power level.

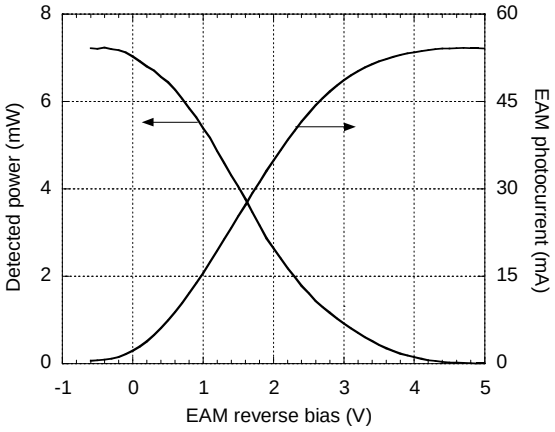

Fig 3: Fiber-coupled transmitted power and EAM photocurrent as a function of EAM reverse bias at 1552 nm.

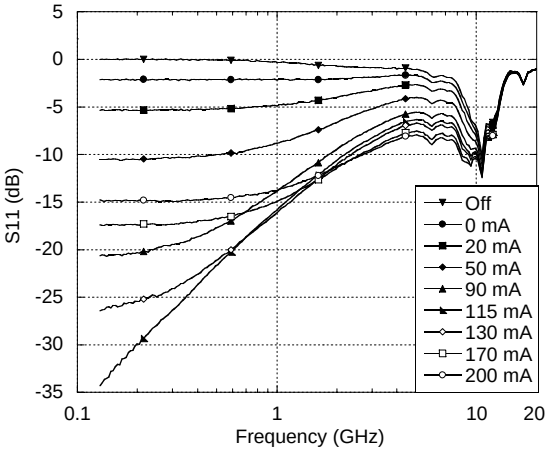

Fig. 4: EAM S11 as a function SOA bias current with 180 mA gain section current.

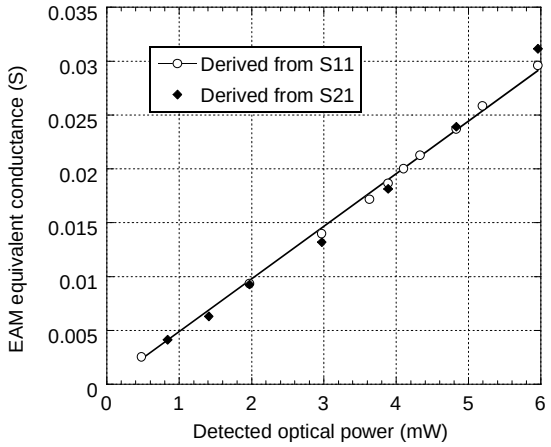

Fig. 5: Equivalent EAM conductance as a function of fiber-coupled transmitted optical power, derived from S–parameters, as a function of fiber-coupled transmitted power.

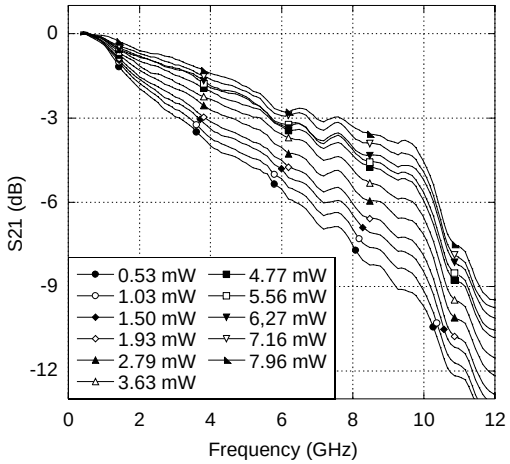

Fig. 6: Measured EAM modulation response for different levels of fiber-coupled transmitted optical power.

The variation of equivalent junction resistance has a large impact on the device performance. It has already been observed that a lower photocurrent can increase the modulation bandwidth by a small amount [2]. Here, because of the large coupled power, the change in 3-dB modulation bandwidth is significant; from 3 GHz at low optical power to closer to 8 GHz at high optical power, illustrated by Fig. 6. The increasing bandwidth can be seen as an effect of compression of modulation sensitivity at lower frequencies due to the reduction of the junction resistance. The compression of the modulation sensitivity can be used to derive the equivalent device conductance and is also shown in Fig. 5. Good agreement is found to what is derived from S11 data.

The compression of the modulation efficiency at lower frequencies is explained by the absorbed photocurrent. In an EAM, the modulation current usually is small and the RF to optical power conversion efficiency can be expressed in the terms of voltage modulation efficiency, dP/dv_m. Here, with the large observed photocurrent, additional information is obtained when the current modulation efficiency, dP/di_m, is taken into consideration. The absorbed photocurrent is directly related to the variation of transmitted optical power and the conversion efficiency related to applied modulation current is therefore fixed at $\eta_i\Gamma$, where η_i is the differential photocurrent detection efficiency and Γ represents optical losses. With the assumption that most modulating sources has a fixed output load termination, often 50Ω, there exists a maximum possible conversion efficiency, not dependent on dP/dv_m, that is limited by the current modulation efficiency, dP/di_m, and the driver output load together with the shunt resistance of the modulator. Figure 7 shows the projected conversion efficiency for the EAM ($dP/dv_m=0.36P_o/Volt$) as a function of coupled input optical power, P_o. A 50Ω RF source, R_S = 7Ω, no optical coupling losses and η_I = 100% have been assumed. The input signal is chosen to be expressed in terms of equivalent source output RF power because of the attribution of total link gain to applied and detected RF power. It is seen in the figure that a potential tenfold increase of waveguide optical power from 20 dBm to 30 dBm will improve the link gain by less than 3dB. The projected performance of an un-terminated and a 50Ω terminated modulator with the same slope-sensitivity, but in the absence of any photocurrent, is also shown in Fig. 7. One path to improve the available gain of the EAM would be to reduce the photocurrent and with that, the differential photocurrent detection efficiency. Clearly, the effects of the absorbed photocurrent represent a fundamental limitation to the available conversion gain of an EAM, used in a high performance analog link application.

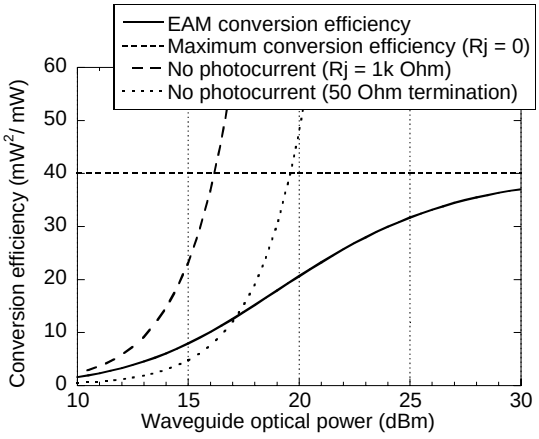

Fig. 7: Modeled electroabsorption modulator conversion efficiency as a function of optical power. The conversion efficiency is related to the output power of a 50Ω output-terminated RF-source.

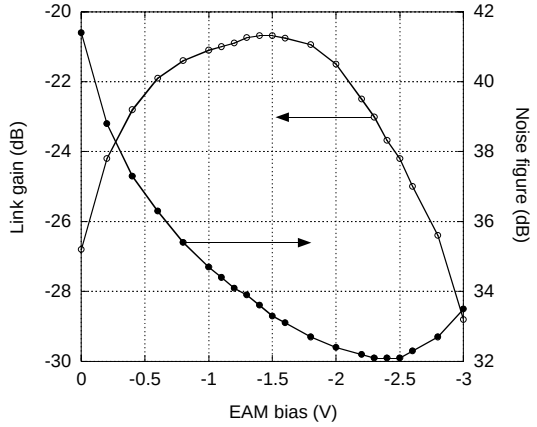

Fig. 8: Link gain and noise figure as a function of EAM bias voltage at 1552 nm for 180 mA gain section bias and 180 mA SOA bias.

Finally, the modulator was used in a simple link demonstration. A 50Ω back-terminated 0.8A/W Discovery photodetector was used at 1 GHz modulation frequency. Figure 8, shows the detected link gain and noise figure as a function of applied bias to the modulator. The equivalent junction resistance is about 30Ω at DC. The link gain peaks at –20.7dB between –1.4V and –1.5V EAM bias voltage. Using the model shown in Fig. 7, increasing the optical power may only improve the EAM conversion efficiency by 4.6 dB, to a maximum attainable link gain of –16.1 dB.

The noise figure reaches its lowest value, 32.1 dB at –2.4 V, different from where the highest gain is found. The reason for the improved noise figure at low bias is found in that for an EAM capable of high extinction and RIN limited noise performance (here RIN is –161.5 dB/Hz at 1 GHz), reducing the bias lower the detected noise power to a higher degree than the gain is reduced. The lowest noise figure is then found at the transition between RIN and shot noise limited operation. This is to the authors knowledge the first time improved link noise figure is demonstrated by 'low biasing' an EAM.

IV. Conclusion

In this paper we have shown how chipscale integration allows coupling of large optical power into a bulk electroabsorption modulator and how this can be used to demonstrate high photocurrent effects in electroabsorption-type modulators. The photocurrent lowers the equivalent junction resistance to less than 30Ω at high optical power, which in turn affects the RF modulation response, both in terms of bandwidth and reflection. It is also shown how with increasing optical power, the RF to optical conversion efficiency will asymptotically approach the behavior of a current-modulated device. Finally, the EAM is applied in a simple link experiment, where it is shown how the noise figure can be improved by 'low biasing' the modulator, compared to the noise figure obtained at the bias point of highest gain.

Acknowledgement

This work was supported by the DARPA RFLICS program via SPAWAR.

References

[1] D.S. Shin, W.X. Chen, S.A. Pappert, D. Chow, D. Yap and P.K.L. Yu, "Analysis of intra-step-barrier quantum wells for high-power electroabsorption modulators," *Int. Topical meeting on Microwave Photonics 2001, MWP '01. 2001*, pp.17–20, 2002.

[2] G.L. Li, W.X. Chen, P.K.L. Yu, C.K. Sun and S.A. Pappert, "The effects of photocurrent on microwave properties of electroabsorption modulators," *1999 IEEE MTT-S International Microwave Symposium Digest*, pp. 1003-1006, 1999.

[3] M.S. Islam, S. Murthy, T. Itoh, M.C. Wu, D. Novak, R.B. Waterhouse, D.L. Sivco, and A.Y. Cho, "Velocity-matched distributed photodetectors and balanced photodetectors with p-i-n photodiodes," *IEEE Trans. Microwave Theory Tech*., **10**, pp. 1914-1920, Oct 2001.

[4] L.A. Johansson, Y.A. Akulova, G.A. Fish and L.A. Coldren, "High optical power electroabsorption wave-guide modulator," *Electron. Lett*., **39**, pp. 364-365, 2003.

[5] Y. A. Akulova, G. A. Fish, P. C. Koh, C. Schow, P. Kozodoy, A. Dahl, S. Nakagawa, M. Larson, M. Mack, T. Strand, C. Coldren, E. Hegblom, S. Penniman, T. Wipiejewski, and L. A. Coldren, "Widely-Tunable Electroabsorption Modulated Sampled Grating DBR Laser Transmitter", *IEEE J. Selec. Top. in Quantum Electron.*, **8**, 1349-1357, Nov/Dec 2002.

[6] G.L. Li, P.K.L. Yu, W.S.C. Chang, K.K. Loi, C.K. Sun and S.A. Pappert, "Concise RF equivalent circuit model for electroabsorption modulators," *Electron. Lett.* **36**, pp. 818-820, 2000.